PFG NMR Study of Diffusion in MFI-Type Zeolites: Evidence of the Existence of Intracrystalline Transport Barriers

ARTICLE *in* THE JOURNAL OF PHYSICAL CHEMISTRY B · MAY 2001

Impact Factor: 3.3 · DOI: 10.1021/jp003899f

PFG NMR Study of Diffusion in MFI-Type Zeolites: Evidence of the Existence of Intracrystalline Transport Barriers

Sergey Vasenkov, Winfried Böhlmann, Petrik Galvosas, Oliver Geier, Hui Liu, and Jörg Kärger*

Universität Leipzig, Fakultät für Physik und Geowissenschaften, Linnéstrasse 5, D-04103 Leipzig, Germany

Received: October 23, 2000; In Final Form: April 2, 2001

The PFG NMR technique is applied to investigate the intracrystalline diffusion of methane and *n*-butane molecules in MFI-type zeolites at several temperatures (from 123 up to 383 K) and over a wide range of diffusion times (from 2 to 35 ms). The intracrystalline self-diffusion coefficients of the guest molecules recorded at low temperatures were observed to decrease with increasing root-mean-square displacements. The comparison of the experimental results with the results of the Monte Carlo simulations of diffusion allowed us to rule out the restriction of diffusion by crystal boundaries as a possible explanation of the observed dependencies of the diffusivities on the root-mean-square displacement. These dependencies are tentatively attributed to the existence of intracrystalline transport barriers in MFI-type crystals. The intersections between the elementary building blocks of the crystals and/or intergrowth sections of MFI crystals are suggested as the possible candidates for the transport barriers.

Introduction

In recent years, MFI-type zeolites have found a wide range of applications. The best known of them include adsorption separation and catalysis. This stimulated investigations of the crystallization mechanism, morphology, and transport properties of MFI crystallites. The numerous studies of the crystallization of zeolites ZSM-5 and silicalite resulted in several models of crystal growth.[1−8] Although these models differ in details, they generally assume that the crystal formation proceeds via one or several stages of aggregation of some primary particles. The size of the aggregating particles was observed to be in the range between several nanometers and tens of nanometers.[1−8] Aggregation of even larger particles (∼350 nm) during crystallization of MFI-type zeolite was recently reported.[2,5] This observation was made using small- and wide-angle X-ray scattering techniques. The insights into the crystallization history of the MFI-type zeolite help to understand the origin of the intergrowth phenomena observed in MFI crystallites.[9−11] Optical examination of large MFI crystals with polarized light often reveals the hourglass structure commonly assigned to the 90° regular intergrowth effects.[10−11] The crystals exhibiting such structure are thought to consist of several components of similar size and of the same microstructure. In addition to the regular 90° intergrowth, the irregular intergrowth effects occurring on a much smaller length scale are also frequently observed.[9]

It may be conjectured that the intersections between different intergrowth components of MFI crystals and/or between the above-discussed building blocks of the crystals may serve as diffusion barriers for guest molecules. Thus, a nonuniform calcination pattern of large MFI crystals reported in ref 11 was attributed to the existence of transport barriers on the internal interfaces dividing different intergrowth sections of the crystals. Here, we report the results of the pulsed field gradient (PFG) NMR investigation of diffusion of small alkanes in silicalite and ZSM-5 crystals. We have observed that at low temperatures the intracrystalline diffusivities progressively decrease with increasing root-mean-square displacements. The observed dependencies are attributed to the existence of intracrystalline transport barriers. Under our experimental conditions, the root-mean-square displacements of the guest molecules were always sufficiently small in comparison with the size of the crystals, so that the effect of diffusion restriction by the outer surface of the crystal was negligible.

Experimental Section

The measurements of self-diffusion of *n*-butane and methane molecules in MFI-type zeolites were carried out using the home-built PFG NMR spectrometer FEGRIS 400 NT operating at a ^{1}H resonance frequency of 400 MHz.[12] For diffusion measurements, the 13-interval bipolar PFG pulse sequence[13] and, in some cases, the standard stimulated echo PFG pulse sequence[14] were used. The former sequence allows us to significantly decrease the disturbing influence of internal magnetic field inhomogeneities on diffusion measurements. These magnetic field inhomogeneities, which are also referred to as internal magnetic field gradients, are induced by the susceptibility variations in heterogeneous samples. An application of magnetic field gradients, which are necessary for PFG NMR diffusion measurements, will inevitably produce a coupling between the applied and internal gradients. As a result, systematic errors in measured diffusivities may occur. The 13-interval PFG pulse sequence makes use of alternating (bipolar) PFGs to reduce the contribution from the cross term between the applied and internal field gradients. Under the condition that over the duration of the measurement the internal gradient remains constant for each spin, the sequence completely eliminates the contribution from this cross term. Such a condition is of particular relevance for the measurements reported in this paper, because the characteristic length scale of constant susceptibility (i.e., the size of the zeolite crystals) was much larger than the molecular displacements over the time of measurements.

* To whom correspondence should be addressed. Phone: +49 341 97 32502. Fax: +49 341 97 32549. E-mail: kaerger@physik.uni-leipzig.de.

10.1021/jp003899f CCC: $20.00
Published on Web 05/31/2001

TABLE 1: Phase Sequence Used for the 13-Interval PFG NMR Sequence

all $\pi/2$, first π	−y	−y	+y	+y	+x	+x	−x	−x	+y	+y	−y	−y	−x	−x	+x	+x
receiver	+x	+x	+x	+x	+y	+y	+y	+y	−x	−x	−x	−x	−y	−y	−y	−y
second π	+x	−x	+y	−y	+y	−y	−x	+x	−x	+x	−y	+y	−y	+y	+x	−x

TABLE 2: Zeolite Samples

sample	zeolite type	Si/Al	mean crystal size/μm^3	supplied by
a	silicalite	> 10^3	120 × 25 × 20	W. Böhlmann, Leipzig
b	silicalite	> 10^3	120 × 30 × 20	W. Böhlmann, Leipzig
c	ZSM-5	79.2	250 × 100 × 100	J. Kornatowski, München

The high performance characteristics of our new PFG NMR spectrometer[12] allowed us for the first time to carry out diffusion measurements in MFI-type zeolites over a wide range of diffusion times (Δ = 2−35 ms) and temperatures (from 123 up to 383 K). To obtain the diffusivity, an attenuation of the PFG NMR spin−echo signal (Ψ) was measured as a function of the amplitude of the applied field gradient (g). For all Δ, the diffusivity was obtained from the initial slope of the ln(Ψ) vs g^2 representation ($-0.8 < \ln(\Psi) < 0$). For the PFG NMR diffusion measurements using the 13-interval sequence, the duration of the applied field gradient pulses (δ) was set to 0.15 or 0.2 ms and the duration of the "dephasing" and the "read" intervals (2τ) was set to 0.6 or 0.8 ms. The time intervals of the stimulated echo sequence were chosen to correspond to those of the 13-interval sequence. Thus, the duration of the applied field gradients was 0.3 ms and the duration of the dephasing and the read intervals was 0.6 ms. The intensity of the applied gradients was varied between 0.1 and 24 T/m for the 13-interval sequence and between 0 and 24 T/m for the stimulated echo sequence. The phase sequence used for the 13-interval PFG NMR sequence is presented in Table 1. The influence of unwanted spin−echo signals on the measurements with the 13-interval sequence was investigated by performing a set of the diffusion measurements of water samples with the known diffusion coefficients. These measurements have shown that under our experimental conditions the unwanted echo signal is suppressed either by the phase sequence or by the applied constant and PFGs.

The diffusion measurements were performed with three different MFI-type samples as specified in Table 2. The zeolite material was supplied in the calcined form.

The samples for the PFG NMR measurements were prepared as follows. The zeolite material (around 300 mg) was introduced into the NMR tube. Then the tube was connected to the vacuum system and the zeolite sample was activated by keeping the zeolite material under high vacuum at 400 C for 20 h. Subsequently, the zeolite sample was loaded with the sorbate gas by freezing the gas from a fixed volume of the vacuum system. Upon loading of the zeolite, the NMR tube was sealed and separated from the vacuum system. The total amount adsorbed corresponded to 1 mmol/g for *n*-butane (samples a and b) and to 1.5 mmol/g for methane (sample c).

The simulations of diffusion were performed using the Monte Carlo method. The random walks were performed on a cubic lattice of size L^3 (L = 200) with periodic boundary conditions. Correlations between different random walkers were neglected, i.e., each path is calculated as if the other random walkers would not exist. The starting points of 1000 random walkers were randomly selected on a lattice. Then the N-step walks ($N \leq 1 \times 10^5$) were generated for each random walker. The final values of the diffusion coefficients reported in this paper were the averages over around 100 lattices with different configurations of the starting points.

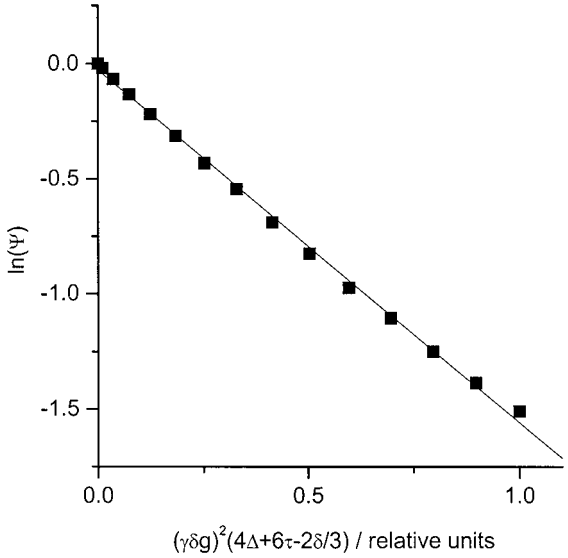

Figure 1. ^{1}H PFG NMR spin−echo attenuation curve for methane in ZSM-5 recorded by using the 13-interval PFG NMR sequence (T = 143 K; Δ = 3 ms).

Results and Discussion

Figure 1 shows an example of the attenuation of the NMR signal (the "spin−echo") of guest molecules in MFI-type zeolite. The attenuation curve was recorded using the 13-interval sequence.[13] The sequence allows us to significantly reduce or completely eliminate the disturbing influence of internal field gradients. When this influence is neglected, the spin−echo attenuation for the 13-interval sequence can be written as[13]

$$\Psi = \exp[-\gamma^2 D\delta^2 g^2(4\Delta + 6\tau - 2/3\delta)] \qquad (1)$$

where γ and D denote the gyromagnetic ratio and the diffusion coefficient. In deriving eq 1, it was assumed that the diffusion can be described by a normal Gaussian propagator

$$P(r,t) = (4\pi Dt)^{-3/2} \exp(-r^2/4Dt) \qquad (2)$$

which represents the probability density for the molecules under study to be displaced over a distance r during a time interval t. For powder samples and when considering sufficiently small signal attenuations, eq 2 is a good approximation even for zeolite crystallites which are known to give rise to anisotropic diffusion like MFI-type zeolites.[15,16] In this case, the diffusivity D

$$D = 1/3(D_x + D_y + D_z) \qquad (3)$$

of eq 2 is in fact one-third of the trace of the diffusion tensor. The validity of this assumption is confirmed by the fact that there are only small deviations of the spin−echo attenuation as represented by Figure 1 from an exponential dependence required by eq 1. In our opinion, these deviations primarily

reflect an occurrence of the diffusion anisotropy. Concentrating only on the initial slope of the attenuation curve, and hence on the mean diffusivity (eq 3), in the present paper these indications of diffusion anisotropy are left out of consideration.

Figure 2a shows the dependencies of the self-diffusion coefficients of *n*-butane on the root-mean-square displacement in silicalite at four different temperatures. The measurements were carried out with the two silicalite samples (a and b). It can be seen in Figure 2a that at low temperatures the diffusion coefficients decrease with increasing root-mean-square displacement. Although a similar trend can also be seen at high temperatures (Figure 2a), the relative change of the diffusion coefficients over similar displacement ranges is much less pronounced at high temperatures than at low temperatures. The measurements were performed using the 13-interval pulse sequence. In addition, at room temperature, the measurements with sample a were also carried out using the standard stimulated echo pulse sequence. It is seen, that the results obtained using both pulse sequences are the same within the experimental uncertainty. This indicates that under our experimental conditions disturbing influences of internal field gradients on the diffusion measurements by PFG NMR are small or nonexistent, even if the measurements are performed using the standard stimulated echo sequence. The results presented in Figure 2a show that in both samples the dependencies of the diffusivities on the root-mean-square displacement as well as their absolute values are almost the same under identical measurement conditions.

Qualitatively, the investigation of the self-diffusion of methane in the ZSM-5 sample c revealed the same results (Figure 2b) as those obtained for the diffusion of *n*-butane in silicalite (Figure 2a). The diffusion coefficients of methane at the low temperatures (133 and 123 K) were found to decrease with increasing root-mean-square displacement. At the same time, at the higher temperatures, the diffusion coefficients of methane were almost independent of the root-mean-square displacements. Thus, in all three different MFI-type zeolites, we observe qualitatively similar dependencies of the diffusivities of the guest molecules on the root-mean-square displacement.

For sufficiently long diffusion times, when the root-mean-square displacements are comparable with the size of the zeolite crystals, the majority of the guest molecules can reach the outer surface of the crystal. In this case, the diffusion coefficient is known to strongly depend on the diffusion time (or the root-mean-square displacement) because of either reflection of guest molecules from the outer surface of the crystals or diffusion out of the crystal.[14] The largest decrease of the diffusion coefficient with increasing diffusion time may be expected in the case of purely reflecting crystal boundaries. Using Monte Carlo simulations, we have estimated the upper limit of this effect on the diffusion coefficients under our experimental conditions and have compared it with the experimentally observed dependencies of the diffusion coefficients on the root-mean-square displacements. The Monte Carlo simulations were carried out using the isotropic approach with an effective diffusivity as given by eq 3. Figure 3 shows the dependence of the diffusion coefficient on the root-mean-square displacement obtained by the Monte Carlo method for diffusion in a cubic lattice of $20 \times 20 \times 20$ μm^3 with purely reflecting boundaries and those recorded by PFG NMR at room temperature for *n*-butane in sample a with the mean crystal size $100 \times 25 \times 20$ μm^3. The latter results feature one of the largest ratios of the root-mean-square displacements to the mean crystal size (Figure 2). Hence, the relative effect of the crystal boundaries on

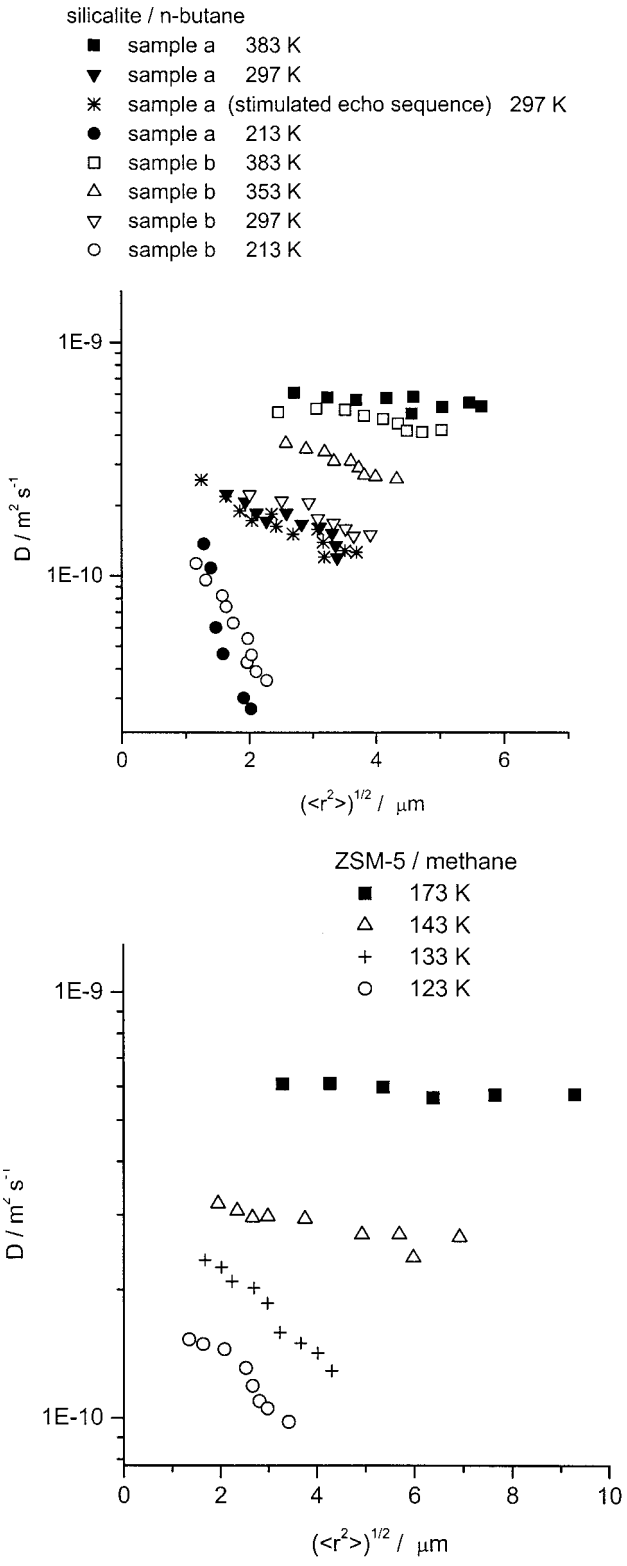

Figure 2. Dependencies of the diffusion coefficients on the root-mean-square displacements measured at different temperatures by the PFG NMR method for (a) *n*-butane in silicalite and (b) methane in ZSM-5. The relative experimental uncertainty of the values of the diffusion coefficients measured in each sample and at each temperature for different root-mean-square displacements does not exceed 10%.

diffusion can be expected to be equally large or even smaller for the rest of the data shown in Figure 2.

The diffusion coefficients of *n*-butane shown in Figure 3 were obtained using eq 1, i.e., using the effective diffusion time Δ_{eff}

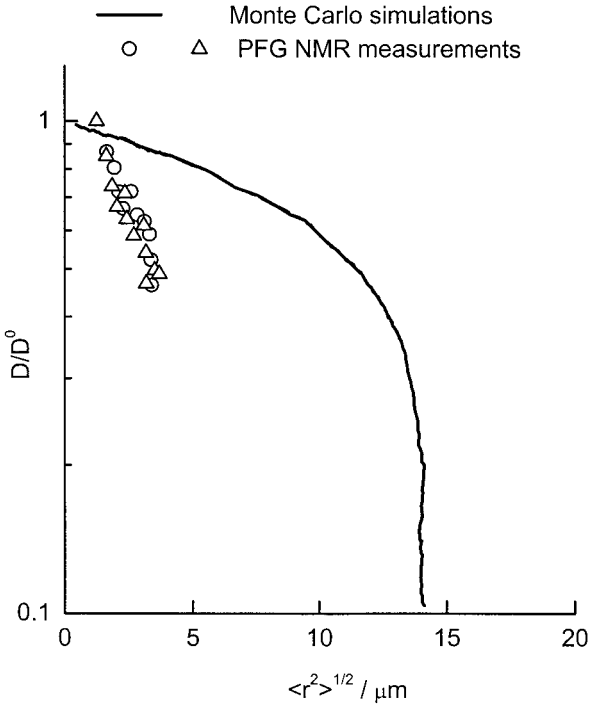

Figure 3. Dependencies of the normalized diffusion coefficients simulated by Monte Carlo method and measured by PFG NMR on the root-mean-square displacements. The points show normalized diffusivities of *n*-butane recorded by PFG NMR in the silicalite sample a at 297 K. The full line shows the results of Monte Carlo simulations of diffusion in a cubic lattice of $20 \times 20 \times 20\ \mu m^3$ with ideally reflecting boundaries. The values of D^0 are equal to the diffusion coefficients obtained at the smallest available root-mean-square displacements, namely, 0.1 μm in the Monte Carlo simulations and 1.24 μm in the PFG NMR measurements.

$= \Delta + {}^3/_2\tau - {}^1/_6\delta$ of the 13-interval sequence as reported by Cotts et al. for the case of unrestricted diffusion.[13] The effect of restricted diffusion during the dephasing and the read intervals changes the effective diffusion time.[17,18] It was shown in ref 18 that for δ and τ not much smaller than Δ the difference between the values of the effective diffusion time for restricted and unrestricted diffusion can be significant. Hence, this difference is of particular consequence when the measurements are performed with small Δ values. For the purpose of the comparison between the simulated and the experimental diffusivities in Figure 3, however, the use of Δ_{eff} for unrestricted diffusion is, in our opinion, well justified in view of the following two items: First, for the smallest Δ values used in our measurements (around 2 ms), Δ is still around 1 order of magnitude larger than δ and around six times larger than τ. Second, for the smallest Δ values and hence for the smallest $\langle r^2 \rangle$ values, the effects of restricted diffusion imposed by the outer surface of the crystal can be expected to be small. This is clearly demonstrated by the comparison of the simulated and the measured diffusivities in Figure 3. For large values of Δ used in our measurements, the difference between Δ and δ (or τ) approaches 2 orders of magnitude. Thus, also in this case, the corrections of Δ_{eff} due to restricted diffusion can be expected to be small. We can conclude, therefore, that the dependencies of the diffusion coefficients on the root-mean-square displacement experimentally observed at the low temperatures cannot be attributed to the restriction of diffusion by crystal boundaries.

The dependence of apparent diffusivities measured by PFG NMR on the root-mean-square displacement might as well be caused by a distribution of the diffusion coefficients of the guest molecules in zeolite.[14] The observation of almost linear attenuation curves (Figure 1), which translates into a single diffusion coefficient via eq 1, as well as the lack of any noticeable distribution of the NMR relaxation times T_1 and T_2 in the studied samples, however, allow us to rule out this explanation of the dependencies shown in Figure 2.

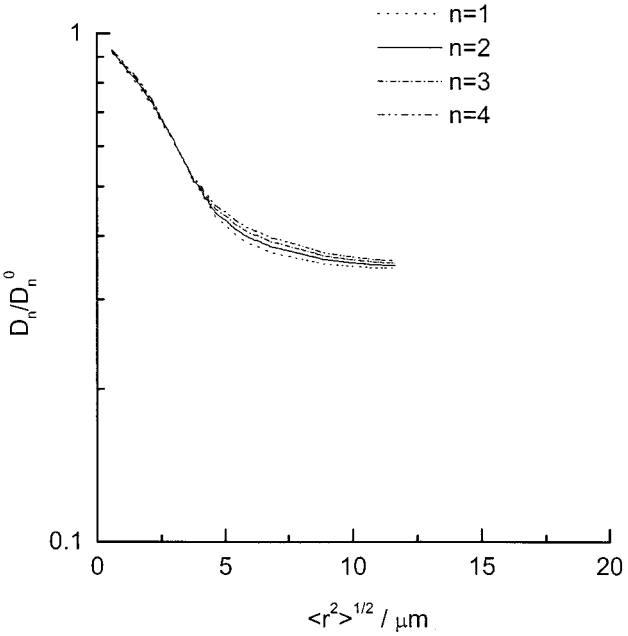

Figure 4. The values of D_n ($n = 1-4$) resulting from the different moments (eqs 3 and 5−7) in dependence on the root-mean-square displacement in a cubic lattice of $5 \times 5 \times 5\ \mu m^3$ with transport barriers on the lattice surface. The probability to pass the barrier is 5×10^{-3} times lower than that of the normal elementary diffusion step in the lattice. Periodic boundary conditions are applied.

Previously reported results of PFG NMR investigation of ethane diffusion in H-ZSM-5 zeolite have also revealed decreasing diffusion coefficients with increasing diffusion time.[19] However, in contrast to the present paper, these results were attributed to the restriction of diffusion by the boundaries of zeolite crystals.[19] By the comparison given in Figure 3, in the present case, this possibility may definitely be ruled out.

In our opinion, there essentially remains only one possibility to explain the observed dependencies (Figure 2), viz., to assign them to the existence of internal transport barriers in MFI-type crystals. As discussed above, the intersections between the building blocks of the crystals and/or intersections between intergrowths sections of the crystals may be considered as possible candidates for internal transport barriers. Covering similar root-mean-square displacements, the relative changes of the diffusivities at low temperatures are found to be much more pronounced than at high temperatures. Such a behavior may be easily explained by assuming that the activation energy of barrier permeation substantially exceeds that of diffusion through the intact zeolite bulk phase. Assuming that the "width" of the diffusion barrier does not significantly exceed one elementary step of diffusion, the experimental dependencies of the diffusion coefficients on the root-mean-square displacements can only be explained if the probability for guest molecules to penetrate such a barrier is orders of magnitude lower than that of diffusion over the same distance during the same time interval in the normal zeolite lattice. This is well illustrated by the Monte Carlo simulations in the cubic lattice ($5 \times 5 \times 5\ \mu m^3$) with periodic boundary conditions (Figure 4). The length of the elementary diffusion step in the simulations was determined by

the size of the simulation system ($200 \times 200 \times 200$) and was equal to 5 μm/200 = 0.025 μm. The probability of the elementary diffusion steps through the lattice boundaries was assumed to be 5×10^{-3} times lower than that of the step in the normal lattice. Periodic boundary conditions ensure that the lattice boundaries correctly reflect the internal transport barriers in the zeolite crystals. The trace with $n = 2$ in Figure 4 shows the ratios D_2/D_2^0 of the diffusion coefficient calculated with transport barriers to that in the same lattice without barriers. The diffusion coefficients were calculated from the second moment of displacement in the lattice using the relation

$$D_2 = 1/6\langle r(t)^2\rangle\frac{1}{t} \tag{4}$$

It is shown in Figure 4 that the diffusion coefficients continuously decrease with increasing root-mean-square displacement when these displacements are lower than, or comparable with, the separation between transport barriers (5 μm). As a consequence of the central limit theorem,[14] for sufficiently large root-mean-square displacements, the diffusion coefficient approaches a constant value. This is reflected by the simulation results (Figure 4). A direct experimental confirmation of this tendency was prohibited by the limitation of the observation times and hence of the molecular displacements accessible during the experiments. There is, however, an obvious tendency that with increasing displacements the dependence of the diffusivities on displacements becomes less pronounced (Figure 2).

Strictly speaking, any internal transport resistance, including the above-discussed internal transport barriers, may lead to deviations from normal diffusion. Only in two cases, namely, for sufficiently small displacements, when the influence of the barriers is negligibly small for the majority of the diffusants and, by virtue of the central limit theorem, for sufficiently large displacements, ideally, normal diffusion shall be approached. The deviations from normal diffusion can be expected to be most pronounced for displacements comparable with the separation between the internal barriers. From PFG NMR studies it appears, however, that in all measurements the PFG NMR signal attenuation is sufficiently well represented by an exponential (eq 1 and Figure 1), so that irrespective of the time dependence of the effective diffusivity, the propagator is well approximated by a Gaussian. To check whether the propagator resulting from the model assumption fulfils this requirement, we have adopted the moment's method as proposed in refs 20 and 21. The method is based on the comparison of the values of D_n resulting from different moments ($n = 1, .., 4$)

$$\langle|\mathrm{r}(t)|^n\rangle = \int|\mathrm{r}(t)|^n\, P(r,t)\, \mathrm{d}r \tag{5}$$

under the assumption that $P(r,t)$ is a Gaussian propagator (eq 2) with D denoting the diffusion coefficient. Using eq 5 and eq 2, we obtain

$$D_1 = (1/16)\pi\langle|r(t)|\rangle^2\frac{1}{t} \tag{6}$$

$$D_3 = \sqrt[3]{\pi/1024}\langle|r(t)|^3\rangle^{2/3}\frac{1}{t} \tag{7}$$

$$D_4 = \sqrt{1/60}\langle|r(t)|^4\rangle^{1/2}\frac{1}{t} \tag{8}$$

The expression for D_2 is given in eq 4. The coincidence of D_n for $n = 1-4$ directly indicate that the propagator is a Gaussian.[20,21] Figure 4 shows that there is no significant difference between the above-discussed D_2 values and the values of D_1, D_3, and D_4 obtained by Monte Carlo simulations for the root-mean-square displacements comparable with the separation between the transport barriers. Hence, we conclude that the diffusion propagators are Gaussian (or almost Gaussian) already in the simplest case considered in our simulations, namely, when there is no distribution of the separations between transport barriers and no distribution in the shape of the areas, restricted by the transport barriers. This result is in agreement with our assumption of the existence of internal transport barriers in MFI-type zeolites.

Diffusion studies of methane and *n*-butane in MFI-type zeolites by the PFG NMR technique are reported in refs 22−25. The comparison of the present data with those previously reported shows general agreement between the absolute values of the diffusion coefficients, extrapolated to the same temperature and diffusion time. In the present work, the supreme capability of our new PFG NMR spectrometer[12] for the first time allowed us to carry out the diffusion measurements in a much broader range of diffusion times and with a significantly better accuracy than in our previous studies.[22−25]

Conclusion

PFG NMR study of diffusion of methane in ZSM-5 and *n*-butane in silicalite at low temperatures reveals diffusion coefficients progressively decreasing with increasing root-mean-square displacements. The measurements were performed using the 13-interval bipolar PFG NMR pulse sequence, which prevents the appearance of systematic errors due to internal magnetic field gradients in the determination of diffusion coefficients. The PFG NMR attenuation curves did not show any indications for the existence of a significant distribution of diffusion coefficients in the investigated zeolites. The comparison of the results of Monte Carlo simulations of diffusion in cubic lattices with the experimental data allowed us to conclude that the observed dependencies of the diffusion coefficients on the root-mean-square displacements cannot be attributed to diffusion restrictions by the outer surface of the zeolite crystals. We tentatively assign these dependencies to the existence of internal transport barriers in crystals of MFI-type zeolite. These internal transport barriers may be attributed to the intersections between the elementary building blocks of the crystals and/or between the crystal intergrowth.

Acknowledgment. We are grateful to Dr. J. Kornatowski for providing us with the sample of ZSM-5 zeolite as well as to the German Science Foundation (the graduate college "Physikalische Chemie der Grenzflächen" and the SFB 294 "Moleküle in Wechselwirkung mit Grenzflächen") and to the Max-Buchner Foundation for financial support.

References and Notes

(1) Regev, O.; Cohen, Y.; Kehat, E.; Talmon, Y. *Zeolites* **1994**, *14*, 314.

(2) De Moor, P.-P. E. A.; Beelen, T. P. M.; Komanschek, B. U.; Diat, O.; van Santen, R. A. *J. Phys. Chem. B* **1997**, *101*, 11077.

(3) Schoeman, B. J. *Zeolites* **1997**, *18*, 97.

(4) Watson, J. N.; Iton, L. E.; Keir, R. I.; Thomas, J. C.; Dowling, T. L.; White, J. W. *J. Phys. Chem. B* **1997**, *101*, 10094.

(5) De Moor, P.-P. E. A.; Beelen, T. P. M.; Komanschek, B. U.; van Santen, R. A. *Microporous Mater.* **1998**, *21*, 263.

(6) Ravishankar, R.; Kirschhock, C. E. A.; Knops-Gerrits, P.-P.; Feijen, E. J. P.; Grobet, P. J.; Vanoppen, P.; De Schryver, F. C.; Miehe, G.; Fuess, H.; Schoeman, B. J.; Jacobs, P. A.; Martens, J. A. *J. Phys. Chem. B* **1999**, *103*, 4960.

(7) Kirschhock, C. E. A.; Ravishankar, R.; Verspeurt, F.; Grobet, P. J.; Jacobs, P. A.; Martens, J. A. *J. Phys. Chem. B* **1999**, *103*, 4965.
(8) Kirschhock, C. E. A.; Ravishankar, R.; Van Looveren, L.; Jacobs, P. A.; Martens, J. A. *J. Phys. Chem. B* **1999**, *103*, 4972.
(9) Hay, D. G.; Jaeger, H.; Wilshier, K. G. *Zeolites* **1990**, *10*, 571.
(10) Weidenthaler, C.; Fischer, R. X.; Shannon, R. D.; Medenbach, O. *J. Phys. Chem.* **1994**, *98*, 12687.
(11) Geus, E. R.; Jansen, J. C.; van Bekkum, H. *Zeolites* **1994**, *14*, 82.
(12) Galvosas, P.; Stallmach, F.; Seiffert, G.; Kärger, J.; Kaess, U.; Majer, G. *J. Magn. Res.* Submitted for publication
(13) Cotts, R. M.; Hoch, M. J. R.; Sun, T.; Markert, J. T. *J. Magn. Reson.* **1989**, *83*, 252.
(14) Kärger, J.; Ruthven, D. M. *Diffusion in Zeolites and Other Microporous Solids*; Wiley: New York, 1992.
(15) Hong, U.; Kärger, J.; Kramer, R.; Pfeifer, H.; Seiffert, G.; Müller, U.; Unger, K. K.; Lück, H.-B.; Ito, T. *Zeolites* **1991**, *11*, 816.
(16) Hong, U.; Kärger, J.; Pfeifer, H.; Müller, U.; Unger, K. K. *Z. Phys. Chem.* **1991**, *173*, 225.
(17) Mitra, P. P.; Halperin, B. I. *J. Magn. Reson. A* **1995**, *113*, 94.
(18) Fordham, E. J.; Mitra, P. P.; Latour, L. L. *J. Magn. Reson. A* **1996**, *121*, 187.
(19) Sorland, G. H.; Aksnes, D.; Gjerdaker, L. *J. Magn. Reson.* **1999**, *137*, 397.
(20) Fritzsche, S.; Haberlandt, R.; Kärger, J.; Pfeifer, H.; Heinzinger, K. *Chem. Phys. Lett.* **1992**, *198*, 283.
(21) Fritzsche, S. *Phase Transitions* **1994**, *52*, 169.
(22) Caro, J.; Bülow, M.; Schirmer, W.; Kärger, J.; Heink, W.; Pfeifer, H. *J. Chem. Soc., Faraday Trans. 1* **1985**, *81*, 2541.
(23) Heink, W.; Kärger, J.; Pfeifer, H.; Datema, K. P.; Nowak, A. K. *J. Chem. Soc., Faraday Trans.* **1992**, *88*, 3505.
(24) Ylstra, W. D.; Kuipers, H. P. C. E.; Post, M. F. M.; Kärger, J. *J. Chem. Soc., Faraday Trans.* **1991**, *87*, 1935.
(25) Snurr, R. Q.; Kärger, J. *J. Phys. Chem. B* **1997**, *101*, 6469.